Available online at www.sciencedirect.com
SCIENCE DIRECT
Polymer 46 (2005) 5165–5182
polymer
www.elsevier.com/locate/polymer

SEC-MALS method for the determination of long-chain branching and long-chain branching distribution in polyethylene

Youlu Yu*, Paul J. DesLauriers, David C. Rohlfing

Chevron Phillips Chemical Company, LP, Bartlesville Research and Technology Center, Bartlesville, OK 74004-0001, USA

Received 21 December 2004; received in revised form 5 April 2005; accepted 11 April 2005
Available online 5 May 2005

Abstract

This paper systematically describes a LCB determination method that can quantify both LCB content and LCB distribution across the molecular weight distribution in polyethylene homopolymers as well as copolymers. Coupling size-exclusion chromatography with multi-angle light scattering (SEC-MALS), this method quantifies molecular weights (MW) and radii of gyration (R_g) simultaneously. The number of LCB per molecule and LCB frequency as a function of MW can be calculated by comparing R_g of a branched polymer with that of a linear control at the same MW using the Zimm–Stockmayer approach. Because the presence of short-chain branching in copolymers results in changes in R_g of the copolymers, their LCB contents cannot be obtained before the short-chain branching (SCB) effect is corrected. Using well-characterized linear PE copolymers as standards, an empirical method is successfully established in this paper to correct the SCB effect. Consequently, this method can be applied to determine LCB in PE copolymers as well. Some practical aspects, such as the selection of formalism for data processing, the LCB detection sensitivity and precision, and long-term reproducibility of this method are also discussed. Finally, examples are given to demonstrate how this method is applied to determine LCB and LCB distribution in practical PE homopolymers and copolymers.

Keywords: Polyethylene (PE); SEC-MALS; Long-chain branching (LCB)

1. Introduction

Long-chain branching (LCB) is a well-known structural phenomenon in polyethylene (PE) [1–5]. Unlike short-chain branching (SCB), LCB in PE can significantly influence the processability and properties of polyethylene resins, even at very low concentrations. Although great progress has been made in understanding the chemical nature and the formation mechanism of LCB, quantitatively characterizing LCB in PE has been a challenging task.

Traditionally, there are three methods for LCB determination, namely, rheology [6–10], nuclear magnetic resonance spectroscopy (NMR) [11], and triple detection SEC (SEC equipped with triple detectors, i.e. a DRI, a viscometer and a low-angle laser light scattering detector) [12]. Of the three methods, rheology and NMR measure the overall average LCB for the full polymer. Triple detection SEC, on the other hand, gives information of LCB distribution across the molecular weight distribution. The theoretical backgrounds on which these three LCB determination methods are based, however, are completely different.

LCB determined via NMR is through a quantitative measurement of peak intensities of side chain methine groups [11]. Inherently, there are two drawbacks associated with the NMR method when used for LCB characterization. First, all branches of six carbons or longer (C_6^+) are quantified by NMR as long branches because NMR cannot resolve methine resonance peaks of the side chains of six carbons or longer. Therefore, LCB content can be overestimated by the method because not all of the C_6^+ side chains are rheologically significant. Furthermore, coupled with low natural abundance of C-13 (1.1%) and inherently low sensitivity, LCB levels in many PE resins are below the NMR detection limit.

Because low levels of LCB in PE can cause dramatic zero-shear viscosity (η_0) increases, rheology has been widely used for diagnosing LCB in PE. There are many rheological methods that have been proposed for LCB

* Corresponding author. Tel.: +1 918 661 9675; fax: +1 918 662 2870.
E-mail address: yuy@cpchem.com (Y. Yu).

0032-3861/$ - see front matter © 2005 Elsevier Ltd. All rights reserved.
doi:10.1016/j.polymer.2005.04.036

quantitation [13–19], the Janzen–Colby [19] model being one of the more successful ones. Janzen and Colby [19] proposed a semi-empirical phenomenological model to quantitatively estimate LCB content in branched polymers based on just their weight-average molecular weights (M_w) and their measured η_0. While having been successfully applied to many PE resins, this method is not without drawbacks: First of all, it is not always easy or even possible to determine accurate η_0 values. η_0 values obtained by extrapolating the complex viscosity $|\eta^*|$–oscillation rate (ω) curve to the zero-shear region is prone to having large errors if the experimental data are not well fit by a mathematical model, such as the Carreau–Yasuda equation [20]. In practice, the $|\eta^*|$–ω curves of some resins in the measurable range show irregular shapes, such as the so-called 'S-shape', while others may be too straight to reliably predict the Newtonian viscosities at the low frequencies. Secondly, the melts of some higher molecular weight polymers, when containing LCB, are extremely stiff such that they cannot be compressed to the required thickness for rheological measurements, making this type of resins unsuitable for LCB characterization with this method. And thirdly, LCB content derived from the Janzen–Colby model is an overall average number for the full polymer. How LCB is distributed across the molecular weight distribution in the polymer is not given by this model.

The Triple detection SEC method, on the other hand, measures the intrinsic viscosity ($[\eta]$) as a function of molecular weight [12,21–23]. By referencing the intrinsic viscosity of a branched polymer ($[\eta_b]$) to that of a linear one ($[\eta_l]$) at the same molecular weight, a relationship between the viscosity branching index factor g' and molecular weight is established. The viscosity branching index factor is defined as:

$$g' \equiv [\eta_b]/[\eta_l] \tag{1}$$

LCB content is then calculated by use of Zimm–Stockmayer equations [24,25]. However, in the Zimm–Stockmayer equations, it is the branching index g (vide infra), not the viscosity branching index g', that has a relationship with the LCB content in branched polymers. The intrinsic viscosity $[\eta]$ of a polymer solution generally does not have a simple relationship with the mean square radius of the polymer in the solution because the 'shielding' effect is almost always present in all polymer solutions [24,26].

To relate the viscosity branching index g' with g, an assumption has to be made, i.e. g' and g have a relationship as shown in Eq. (2).

$$g' = g^{\varepsilon} \tag{2}$$

where ε is the so-called drainage factor, which depends on the type of LCB and the solvent quality, etc. [27,28]. Unfortunately, the value of ε is often found not to be a constant across the molecular weight distribution. Although theoretical value of ε is in the range of 0.5–1.5 [24,25], numbers beyond this range have also been reported [29]. Therefore, in practice, dramatically different LCB contents for a same resin can result simply because of the choices of ε values. The molecular weight dependence of ε makes the matter even more complicated.

SEC-MALS is a technique that combines of size-exclusion chromatography (SEC) with multi-angle light scattering (MALS). Because this method can determine the absolute molecular weight and root-mean-square (RMS) radius (also known as radius of gyration, R_g) simultaneously, branched polymers can be characterized with this technique by direct application of the Zimm–Stockmayer approach [24,25]. Many researchers have used SEC-MALS at the ambient temperature for the characterization of branched polymers, such as polystyrene and poly(methyl methacrylate) type of branched polymers [30–35]. Although the application of high temperature SEC-MALS to characterize polyethylenes has also gained momentum in recent years [36–43], it is largely limited to PE homopolymers—reports on determination of LCB in PE copolymers via the SEC-MALS method are very scarce. Furthermore, to the best of our knowledge, there is no systematical study can be found in the literature that deals with the practical aspects in the high temperature SEC-MALS method for the determination of LCB in PE resins. In this paper, we describe an empirical method for the correction of the short-chain branching effect on the LCB determination in PE copolymers. A systematical study on the practical aspects, such as mathematical formalism selection for data processing, the detection sensitivity and the detection precision, and long-term stability and reproducibility, etc. is also thoroughly described. At the end of this paper, examples are given to demonstrate how this technique is applied to determine LCB level and LCB distribution across the MWD (LCBD) in practical PE hopolymers and copolymers.

2. Experimental

Fig. 1 is a schematic plot of a SEC-MALS system, where SEC-MALS is a combined method of size exclusion

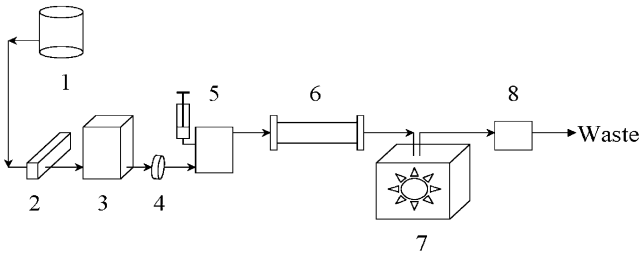

Fig. 1. A schematic plot of SEC-MALS set-up.

chromatography (SEC), also known as gel-permeation chromatography (GPC), with multi-angle light scattering (MALS). In the SEC-MALS system, a DAWN EOS photometer (Wyatt Technology, Santa Barbara, CA) is attached to a Waters 150-CV plus GPC system (Milford, MA) or a PL-210 GPC system (Polymer Labs, UK) through a hot-transfer line controlled at 145 °C. As shown in Fig. 1, degassed mobile phase, 1,2,4-trichlorobenzene (TCB), containing 0.5 wt% of BHT is pumped through an inline filter before passing through the SEC column bank. Polymer solutions injected to the system are brought downstream to the columns by the mobile phase for fractionation. The fractionated polymers first elute through the MALS photometer where light scattering signals are recorded before passing through the differential refractive index detector (DRI) where their concentrations are quantified.

The DAWN EOS system was calibrated with neat toluene at room temperature to convert the measured voltage to intensity of scattered light. During the calibration, toluene was filtered with a 0.02 μm filter (Whatman) and directly passed through the flowcell of the EOS system. At room temperature, the Rayleigh ratio at the given conditions is given by $1.406\times10^{-5}\,\mathrm{cm}^{-1}$ [44]. A narrow polystyrene (PS) standard (American Polymer Standards) with MW of 30,000 g/mol and a concentration of 5–10 mg/ml in TCB was employed to normalize the system at 145 °C. At the given chromatographic conditions, the radius of gyration (R_g) of the polystyrene (PS) was estimated to be 5.6 nm using the Fox–Flory equation coupled with its Mark–Houwink exponent in the chromatographic conditions [45,46].

The differential refractive index detector (DRI) of the Waters GPC instrument was calibrated with a known quantity of a PE standard injected to the column. By averaging the total chromatographic areas of recorded chromatograms for at least five injections, the DRI constant (α_{RI}) was obtained since the sensitivity of the DRI detector is directly proportional to the product of polymer concentration and the refractive index increment (dn/dc) of PE in TCB at the measuring temperature as described in Eq. (3).

$$\alpha_{RI} = \frac{\left(\frac{dn}{dc}\right)c}{I_{RI}} \tag{3}$$

where I_{RI} is the output intensity of the DRI detector.

At a flow rate set at 0.7 ml/min (actual flow rate: 0.60–0.65 ml/min), the mobile phase was eluted through three (3) 7.5 mm×300 mm 20 μm mixed A columns (Polymer Labs, UK). PE solutions with nominal concentrations of 1.0–1.2 mg/ml were prepared at 150 °C for 3–4 h before transferred to SEC injection vials sitting in the carousel heated at 145 °C. In addition to a concentration chromatogram, seventeen light scattering chromatograms at different angles were also acquired for each injection. At each chromatographic slice, both the absolute molecular weight (M) and the root mean square radius, also known as radius of gyration, R_g, were obtained from Debye plots [30]. The linear PE control employed in this study was HiD9640, a high density PE with broad MWD (Chevron Phillips Chemical). The manufacturer-suggested refractive index increment dn/dc value for PE dissolved in TCB at 135 °C is 0.097 ml/g. Using this dn/dc number, we found that the measured M_w of SRM1475 agreed very well with the certified number by NIST [47]. We thus adopted the manufacturer-suggested dn/dc value in this work [48].

3. Theoretical background

3.1. Relationships between scattered light and molecular weight and size

From the fundamental light scattering theory [49–51], the intensity of scattered light from a dilute polymer solution can be described by Eq. (4):

$$\frac{R_\theta}{Kc} = MP(\theta)(1 - 2A_2cMP(\theta) + \ldots) \tag{4}$$

where R_θ is the excess Rayleigh ratio, the ratio of the scattered and incident light intensity; M is the molecular weight of the polymer. If the polymer is non-uniform, it should be the weight-average molecular weight, M_w; c is the concentration of the polymer; A_2 is the second virial coefficient, a thermodynamic term; $P(\theta)$ is an angular dependent scattering function; and K is a constant.

For vertically polarized incident laser light, K is given by Eq. (5):

$$K = \frac{4\pi^2 n_0^2}{N_A\lambda_0^4}\left[\frac{dn}{dc}\right]^2 \tag{5}$$

where n_0 is the refractive index of the solvent; N_A is Avogadro's number; λ_0 is the wavelength of the laser beam in vacuum; and dn/dc is differential refractive index increment of the polymer in the specific solvent at the run temperature.

$P(\theta)$ describes the angular dependence on the intensity of scattered light. The definition of the particle scattering function is:

$$P(\theta) = \frac{R_\theta}{R_0} \tag{6}$$

where R_θ and R_0 are the excess Rayleigh ratios at the observation angle θ and zero, respectively. For small molecules whose sizes are smaller than ca. $\lambda/20$, the intensity of scattered light is independent of the scattering angle, so that $P(\theta)=1$ for all angles. For larger particles, however, $P(\theta)$ is a function of scattering angles and can be described by Eq. (7):

$$P(\theta) = 1 - \frac{16\pi^2}{3\lambda^2}\sin^2\left(\frac{\theta}{2}\right)\langle R_g^2\rangle + \text{higher order} \tag{7}$$

As the scattering angle approaches to zero, i.e. $\theta \rightarrow 0$, the higher order in Eq. (7) can be neglected. The following equation (Eq. (8)) holds:

$$P^{-1}(\theta) = 1 + \frac{16\pi^2}{3\lambda^2}\sin^2\left(\frac{\theta}{2}\right)\langle R_g^2\rangle \tag{8}$$

where λ is the wavelength of the incident light in a given solvent ($\lambda = \lambda_0/n_0$); R_g is the root mean square (RMS) radius, or radius of gyration (R_g), of the scattering particle. It should be noted that R_g describes the size of a macromolecule in the solution regardless of its shape; it is not identical with the geometrical radius. For flexible polymer chains in solution, each conformation has an R_g. However only the average of R_g over all conformations has the practical meaning.

3.2. Debye formalism vs. Zimm formalism

Eq. (4) is the very basic equation in light scattering, from which molecular weight (again, in case of the non-uniform polymer, the weight-average molecular weight, M_w) and R_g can be obtained through a Debye plot, that is, a plot of R_θ/Kc vs. $\sin^2(\theta/2)$. By fitting a polynomial in $\sin^2(\theta/2)$ to the data, both the intercept ($R_0/K\,c$) and the slope (σ_0) at the zero angle $\sigma_0 \equiv d(R_\theta/Kc)/\mathrm{d}(\sin^2(\theta/2))_{\theta\rightarrow 0}$ can be obtained. Please note that, as θ approaches zero, the particle scattering function $P(\theta)$ approaches to unity. Therefore Eq. (4) becomes:

$$\frac{R_{\theta\rightarrow 0}}{Kc} = \frac{R_0}{Kc} = M - 2A_2cM^2 \tag{9}$$

If $A_2 = 0$, then

$$M = \frac{R_0}{Kc} \tag{10}$$

Otherwise, solving Eq. (9) yields M.

To find R_g, the first two terms in Eq. (7) are substituted into Eq. (4). The higher order terms in Eq. (4) may be neglected when concentration is very low, which is the case for the chromatographic conditions. The following equation is obtained:

$$R_g = \left(\frac{-3\sigma_0\lambda^2}{16\pi^2 M(1 - 4A_2Mc)}\right)^{0.5} \tag{11}$$

Fig. 2 shows the Debye plots of the linear control at the given molecular weight (or elution volume) with Fig. 2(A) being the lowest MW (largest elution volume) and Fig. 2(D) the highest (smallest elution volume). It is evident in Fig. 2 that the Debye plots with the Debye formalism (Eq. (4)) resulted in non-linear curves, especially for the higher molecular weights. Therefore, a higher order of polynomial was needed for data fitting in order to obtain the intercept and slope at the zero-angle. However, a higher order polynomial resulted in a very unreliable slope at the zero-angle because light scattering data fluctuation at the lower angle is always relatively larger than that at the higher scattering angle. Consequently, normal scattering data fluctuation was found to cause dramatic variations in R_g deduced from Eq. (11), especially for the lower MW.

Eq. (4) may also be put into a reciprocal form, or called the Zimm formalism:

$$\frac{Kc}{R_\theta} = \frac{1}{MP(\theta)} + 2A_2c + \ldots \tag{12}$$

Inserting Eq. (8) into Eq. (12) results in Eq. (13).

$$\frac{Kc}{R_\theta} = \frac{1}{M}\left(1 + \frac{16\pi^2}{3\lambda^2}\sin^2\left(\frac{\theta}{2}\right)\langle R_g^2\rangle\right) + 2A_2c + \ldots \tag{13}$$

A plot of $K\,c/R_\theta$ vs. $\sin^2(\theta/2)$, or Debye plot with Zimm formalism, yields a straight line, from which both M and R_g are obtained, again, from the reciprocal of intercept and the slope ($\sigma_0 \equiv \mathrm{d}(Kc/R_\theta)/\mathrm{d}(\sin^2(\theta/2))_{\theta\rightarrow 0}$) at the zero angle.

In the Debye plot with Zimm formalism case,

$$M = \left(\frac{Kc}{R_0} - 2A_2c\right)^{-1} \tag{14}$$

and

$$R_g = \left(\frac{3\sigma_0\lambda^2 M}{16\pi^2}\right)^{0.5} \tag{15}$$

Debye plots with Zimm formalism were found to be largely linear over practically the entire molecular weight range. Fig. 3 shows the same slices as those shown in Fig. 2 except the Zimm formalism was used. Clearly, linear relationships were found for all of these slices. In fact, the linear relationship was found for practically the entire molecular weight range. Therefore, all data presented in this report were obtained from Debye plots with Zimm formalism using the first order polynomial (or straight line) in $\sin^2(\theta/2)$ for data fitting.

4. Results and discussion

4.1. Selection of chromatographic region for R_g–MW plot

Fig. 4 shows an overlay of R_g and MW as a function of elution volume. The raw concentration (DRI) and 90° light scattering chromatograms are also superimposed on it. As expected, at the low elution volume end (or the high MW end), because of the poor signal/noise ratios (S/N) for the concentration chromatogram, large data fluctuations were found for both R_g and MW. As the elution volume increased, R_g and MW were found to follow well-defined lines. For further increases of the elution volume, however, the R_g, and then the MW data became scattered again. This is because as the elution volume increases (or the molecular weight decreases) to a point that the sizes of the polymer molecules in the solution are small enough such that the particle scattering function $P(\theta)$ becomes unity, the scattered light is no longer angular-dependent. At this

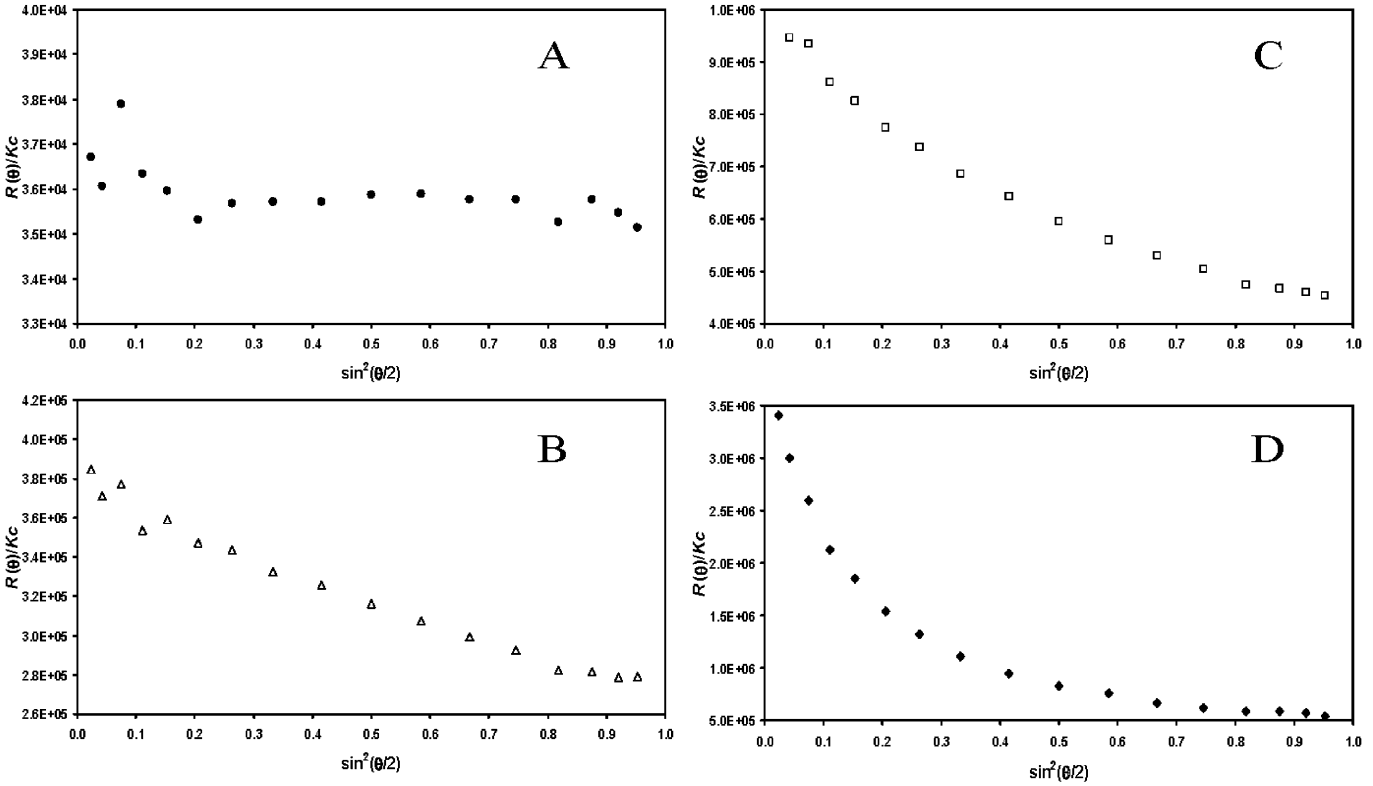

Fig. 2. Debye plots with Debye formalism for SEC slices taken at different elution volumes (or molecular weights) from a chromatogram of the linear control. Molecular weight increases in the order of A to D. The non-linearity is evident for the higher molecular weight slices.

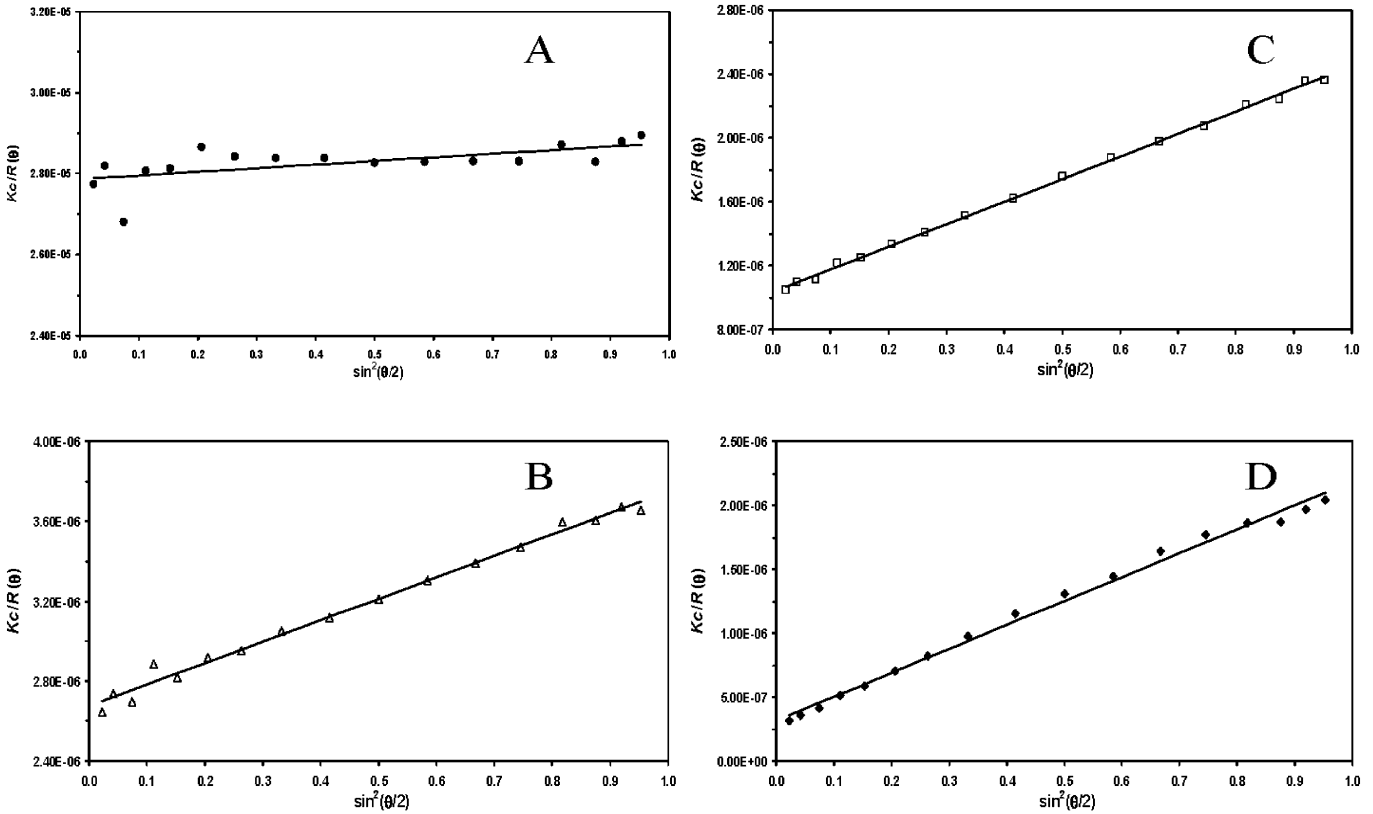

Fig. 3. Debye plots with Zimm formalism for the same SEC slices as shown in Fig. 2, where the solid lines are the first-order polynomial (linear) fitting lines. A linear relationship is evident for all of these slices.

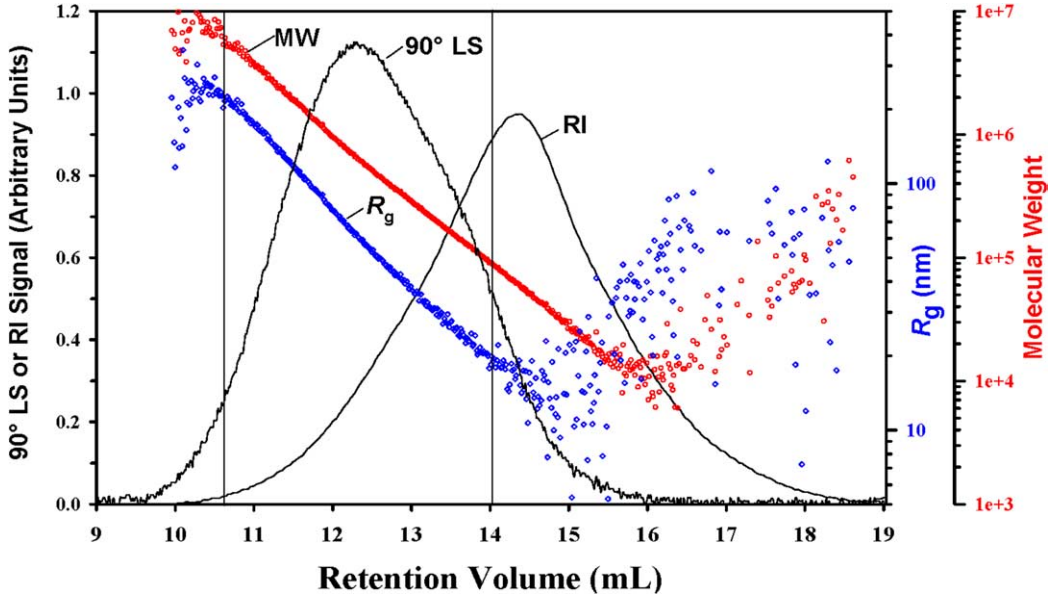

Fig. 4. An overlay of molecular weight and radius of gyration R_g as a function of elution volume. The two vertical lines define the region used to take the values of R_g and MW for long-chain branching calculation.

point, even though both the DRI and LS signals were strong for a given chromatographic slice, no meaningful slope of the Debye plot could be obtained, resulting in meaningless R_g values. Keep in mind that the minimum measurable size of a polymer is determined by the wavelength of the laser employed. For the laser employed in this study (690 nm), the minimum measurable size is, according to the manufacturer of the instrument, ca. 10 nm.

The intensity of scattered light is proportional to the product of polymer concentration, c, and polymer molecular weight, M. Given that the molecular weight decreases exponentially as the elution volume increases and that the concentrations of polymer solutions were kept low under the chromatographic conditions in order to avoid column overloading and flow problems, the product of Mc becomes diminishingly small for further increases of elution volumes, resulting in meaningless M values, in keeping with the observation in Fig. 4.

To have both reliable R_g and MW for long-chain branching (LCB) calculation, only high confidence R_g and MW data points were selected for LCB calculations in this study. As an example, R_g–MW data plotted in Fig. 5 were selected from the region defined by the two vertical bars in Fig. 4, within which the uncertainties in both R_g and MW data points were minimum.

4.2. Calculation of long-chain branching

The Zimm–Stockmayer approach [24] was employed to determine the amount of LCB in polyethylene resins in this report. As discussed above, in SEC-MALS both M and R_g are measured simultaneously at each slice of a chromatogram. At the same molecular weight, R_g of a branched polymer is smaller than that of a linear one. To convert the R_g–M relationship into LCB–MW for the branched polymer, the branching index (g) factor, which is defined as the ratio of the mean square radius of gyration of branched polymer to that of linear one at the same molecular weight (Eq. (16)), needs to be determined first.

$$g \equiv \left(\frac{\langle R_g^2 \rangle_b}{\langle R_g^2 \rangle_l} \right)_M \tag{16}$$

where the subscripts b and l represent the branched and linear polymer, respectively.

Zimm and Stockmayer demonstrated that for any randomly branched polymers whose branches are tri-functional (or Y-shaped) and randomly distributed in length, the branching index of this type of branched polymer (g_{3w}) and the weight-average number of LCB per molecule (B_{3w}) have a relationship as shown in Eq. (17a).

$$g_{3w} = \frac{6}{B_{3w}} \left\{ \frac{1}{2} \left(\frac{2 + B_{3w}}{B_{3w}} \right)^{1/2} \ln \left[\frac{(2 + B_{3w})^{1/2} + (B_{3w})^{1/2}}{(2 + B_{3w})^{1/2} - (B_{3w})^{1/2}} \right] - 1 \right\} \tag{17a}$$

For polymer having tetra-functional branches with random length distribution, its branch index (g_{4w}) and the weight-average number of branches per molecule (B_{4w}) have the following relationship (Eq. (17b)):

$$g_{4w} = \frac{1}{B_{4w}} \ln(1 + B_{4w}) \tag{17b}$$

Eqs. (17a) and (17b) in principle also apply to polydispersed polymers. But in such cases, the z-average molecular weights (M_z) have to be known [24]. This, however, rarely is the case for SEC slices. Fortunately,

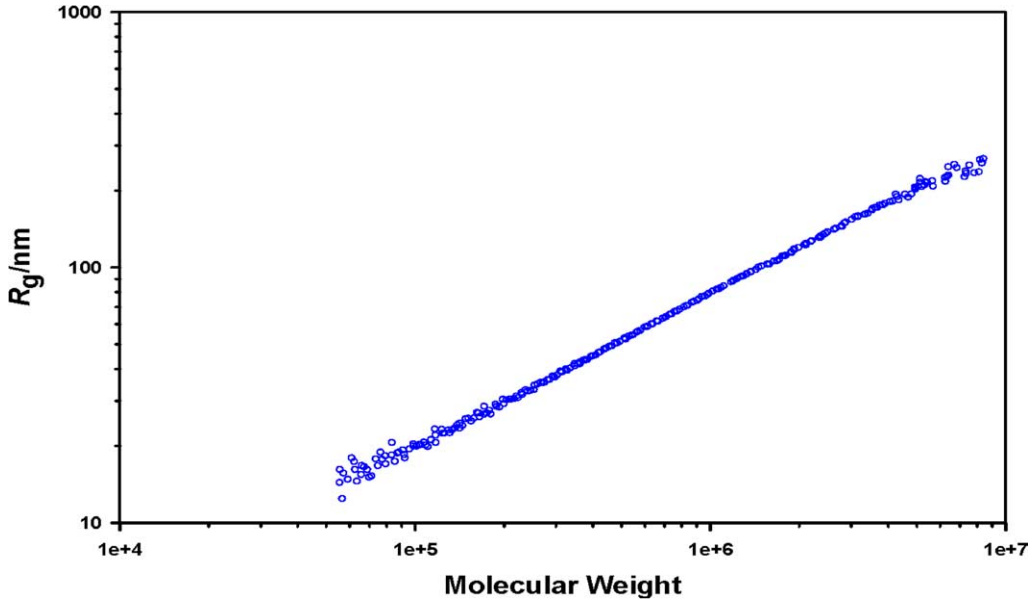

Fig. 5. The relationship of radius of gyration (R_g) and molecular weight for the linear control using the data selected from the region defined by the two vertical lines in Fig. 4.

under the chromatographic conditions, the polydispersity of each SEC slice under the proper conditions is so small that the ratio of each slice is close to unity. Therefore, M_w and M_z may be treated as the same.

LCB frequency (λ_{M_i}), or number of LCB per 1000 carbons, of the *i*th slice in a chromatogram can be calculated straightforwardly with Eq. (18) using the value of B (number of LCB per molecule, B_{3w} or B_{4w} for tri- or tetra-functional, respectively) obtained from Eq. (17).

$$\lambda_{M_i} = 1000 M_0 B / M_i \tag{18}$$

where M_0 is the unit molecular weight, for polyethylene, $M_0 = 14$; and M_i is the MW of the *i*th slice. The LCB distribution across the MWD (LCBD) for a polymer can thus be established using Eqs. (17) and (18). Please note that, since the functionality of LCB in PE as revealed by NMR [9,11] is tri-functional, we will limit the discussion in the following to the tri-functional case.

Figs. 6 and 7 present the simulated results using Eqs. (17a) and (18). Since all the relationships among MW, g_{3w}, and LCB frequencies are described by Eqs. (17a) and (18), Figs. 6 and 7 provide pictorial views to show how these three parameters are inter-related. In Fig. 6, R_g is plotted against MW at various fixed LCB levels. The data points presented in the figure were experimentally determined for the linear control [52]. As the LCB levels in the simulated branched polymer chains increase, the negative deviation of R_g compared to the linear control becomes more pronounced. The higher the LCB content in a branched polymer, the larger the negative deviation of R_g.

Fig. 7 shows how g_{3w} decreases as the LCB content increases in branched polymers at fixed molecular weights. After examining Fig. 7 carefully, the following may be said: with the same branching index g_{3w}, the LCB frequency in a high MW is lower than that in a low MW; on the other hand, at the same LCB content, the branching index g_{3w} of a high MW polymer is smaller than that of a low MW polymers.

Both Figs. 6 and 7 suggest that, for the same LCB frequency, while LCB may be detected at a high MW, the same is not necessarily true at a low MW. For example, at a LCB level of 0.01 LCB/1000 carbons, while SEC-MALS can unmistakably detect the presence of LCB for molecular weights equal to or greater than 1,000,000 g/mol, the same cannot be said for molecular weights 200,000 g/mol or smaller.

4.3. LCB detection limit and LCB detection background

Fig. 6 can also be used to estimate the LCB detection limit by the SEC-MALS method described above. In practice, strictly linear polyethylene (PE) samples rarely exist. Polyethylene prepared through anionic polymerization of butadiene followed by hydrogenation, although it may not contain LCB, still contains some ethyl side chains [53–56]. Furthermore, LCB polymer standards with known levels of LCB and clear architectures are hardly available. Given the lack of LCB standard samples, it is impossible to experimentally determine the LCB detection limit. However, using Fig. 6, the LCB detection limit can be estimated graphically.

The LCB detection limit was found to be MW dependent. As can be seen in Fig. 6, as the LCB level in branched polymers decreases, the R_g–MW relationship of the branched polymers become closer to that of the linear control. For MW being equal to or greater than 1,000,000 g/mol, for example, for the LCB levels lower than 5E-6, R_g–MW of the

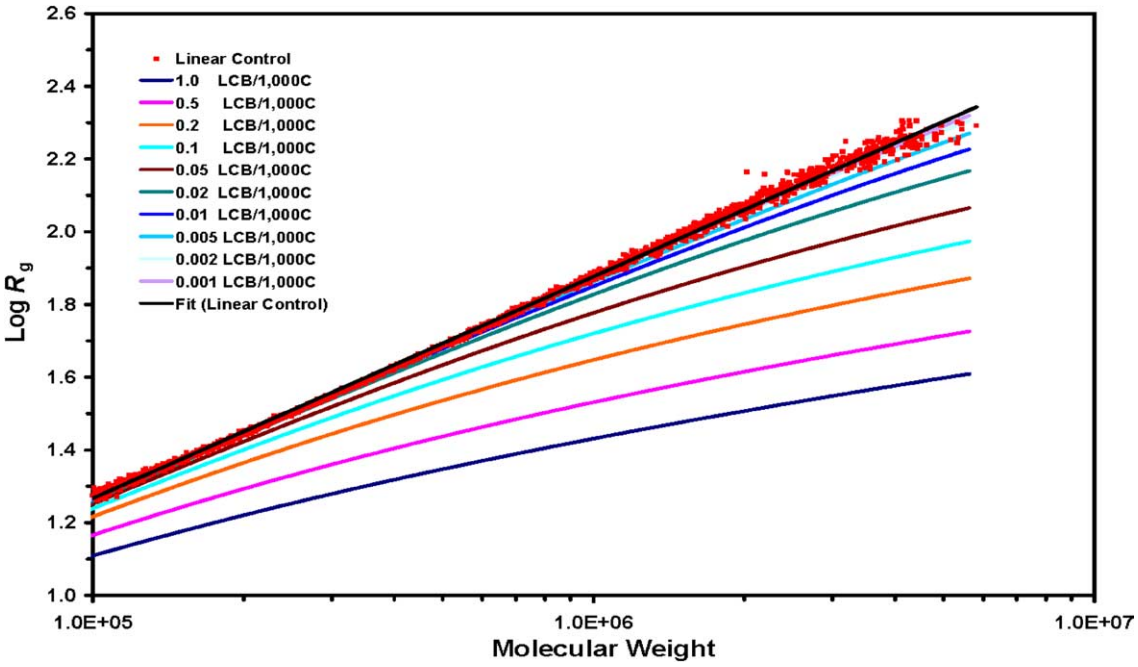

Fig. 6. Simulated relationships of radius of gyration (R_g) and molecular weight for branched polymers with various long-chain branching levels.

branched polymer starts to overlap with that of the linear control. This means that SEC-MALS cannot confidently quantify LCB at that level for that molecular weight. In other words, the LCB detection level is near 0.005 LCB/1000 carbons (or 5E-6) for PE of MW equal to or greater than 1,000,000 g/mol. As the MW decreases, the LCB detection level becomes increasingly poorer.

Like any other physical measurements, the measured g_{3w}–M relationship that was used for LCB calculation was not without data fluctuation. In addition to the conventional chromatographic conditions, such as the stability of temperature and/or flowrate, etc. that could affect the data quality, the cleanness of the solvent (free from particulates) can also result in deterioration of light scattering data quality. As such, referencing the linear control against itself in replicate runs resulted in a residual LCB distribution across the MWD. This residual LCB is called the LCB detection background (the background) in this paper.

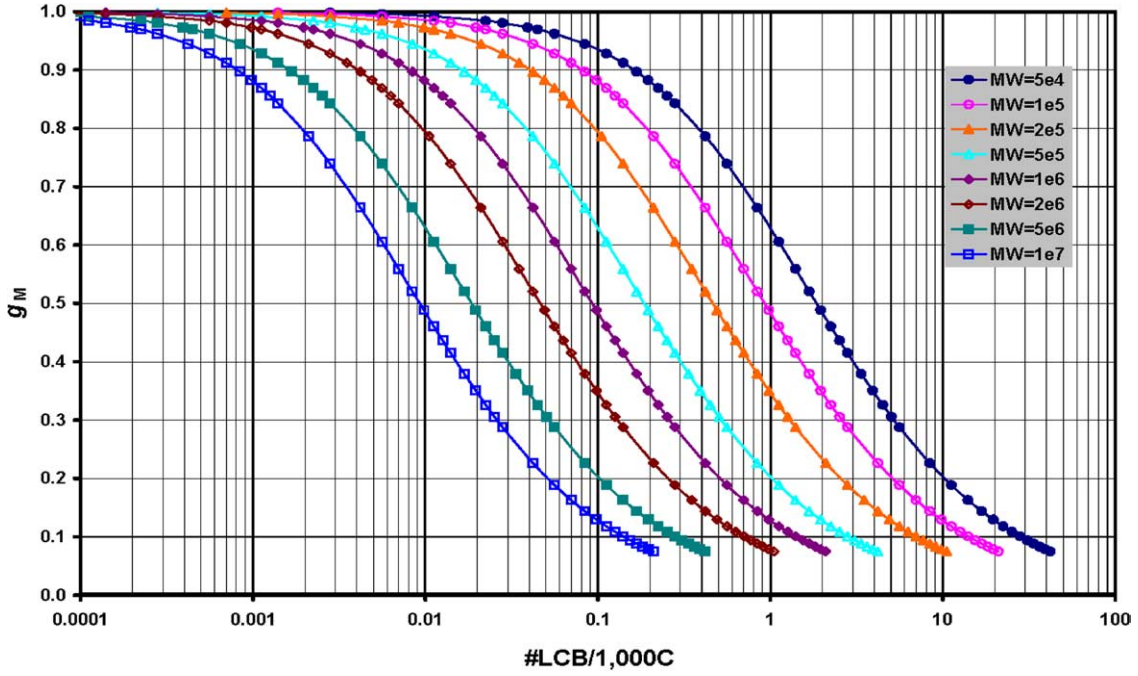

Fig. 7. Simulated relationships between branching index (g_{3w}) and long-chain branching frequency for branched polymers at various molecular weights.

A typical plot of the LCB detection background as a function of molecular weight is shown in Fig. 8. The background was found to be generally low, mostly below 0.005 LCB/1000 carbons (5E-6) for higher MW but to increase rapidly as the molecular weight become smaller than 200,000 g/mol. This is consistent with the fact that the uncertainty in R_g for MW smaller than 200,000 g/mol also increases rapidly for both of the linear control and branched polymers. It may be worth mentioning that the measured LCB level at or below the background is not meaningful.

4.4. R_g reproducibility and long-term stability

Reproducibility here is defined as the variability of the measured R_g–MW relationships for replicates within the same experimental batch, generally within 24 h. As can be seen in Fig. 9, it is evident that the reproducibility of these runs is excellent. Plotted in Fig. 9 are the R_g–MW relationships for the linear control sample for multiple runs in the same batch within 24 h. All the R_g data points in the figure seem to follow very well with the same line across the molecular weight distribution except at the two ends, at which there seems to be slightly more scatter in the data. This increased data scatter at the two ends may be explained by the following: at the low MW side (say, MW < 100,000 g/mol), the R_g of the particles is so small that their angular dependence is intrinsically weak. Any normal data fluctuation can result in significant changes in the slopes of the Debye plots, resulting in additional fluctuation in R_g. At the high MW end, however, although the size of the polymer can be measured very accurately, there are larger uncertainties in the measured molecular weights due to poor *S*/*N* in the concentration signals at the high MW end.

Long-term stability, on the other hand, is defined as the variability of the measured R_g–MW relationships for the same sample run over a much longer period of time, covering months or even years. The R_g–MW plots for the same linear control measured over a period of 18 months are shown in Fig. 10. Approximately three months separated each measurement. During this period, the SEC-MALS system experienced almost all kinds of chromatographic conditions changes, including column changes, DRI detector replacement, light-scattering detector flowcell cleaning and replacement, and pump replacement, to name a few. Of course all these impacted the measured R_g–MW relationships. Although the overall line-width of R_g–MW in Fig. 10 is perhaps broader than that in Fig. 9, the general shapes of the R_g–MW plots in Figs. 9 and 10 remain unchanged. The long-term stability of the SEC-MALS method seems to be very good over an eighteen-month period of time.

Higher relative errors, however, were observed at the lower MW end, where R_g curved upward (Fig. 10). Since solution concentration, column loading, and flowrate were kept practically unchanged over the period of time, it is believed that this R_g–MW upward curvature at the low MW end was mainly caused by column aging or a dirty flowcell resulting from coating on the surface of the cell (on windows or bore) over time. On aged columns, co-elution of large and small polymers could occur due to a deteriorated fractionation efficiency of the aged columns. Consequently, the apparent R_g thus measured would be larger than that measured with newer columns at the same molecular

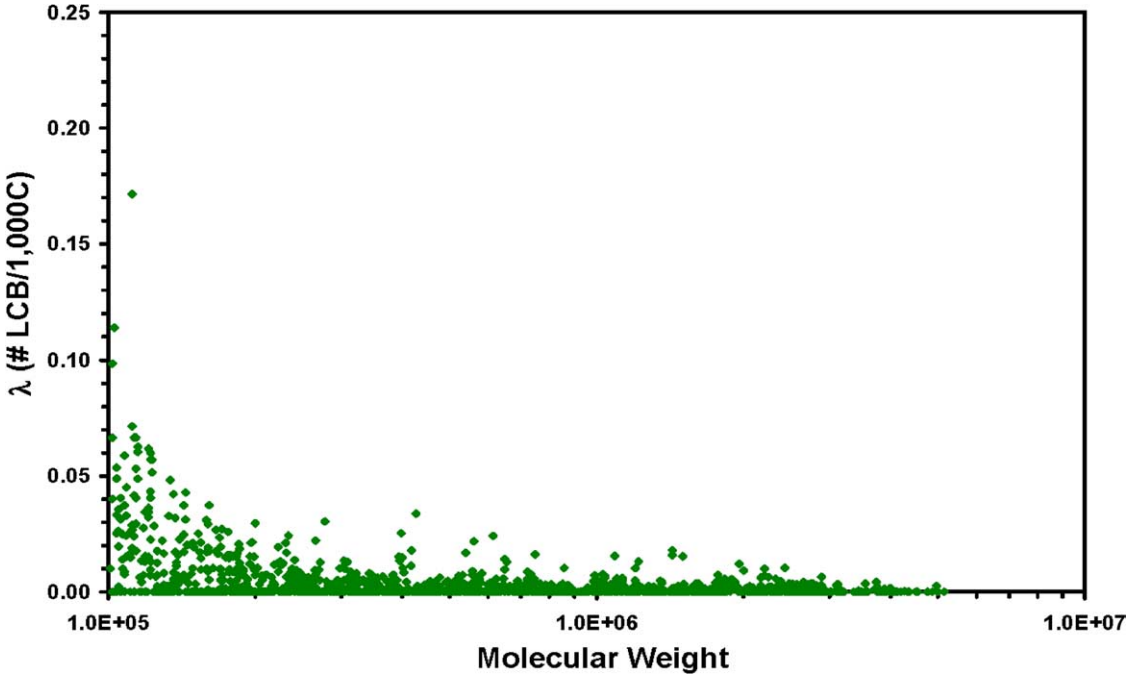

Fig. 8. A typical plot of the LCB detection background as a function of molecular weight.

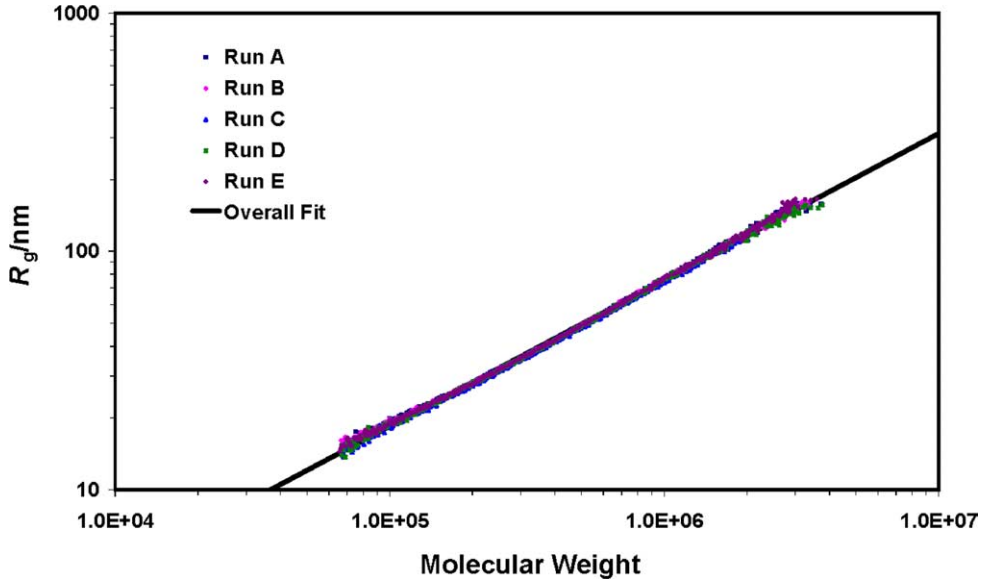

Fig. 9. The relationships of radius of gyration (R_g) and molecular weight for the linear control of replicate runs in the same batch within 24 h.

weight, resulting in R_g–MW upward curvature at the low MW end because the detected radii of gyration are z-average numbers that are biased towards the larger polymers [30,35]. On the other hand, the gradual deposition of a coating onto the flowcell can result in 'stray light' which could cause the cell background signal to increase. Although this may not result in significant relative errors in R_g for high MW, it could for low MW. Therefore, in addition to timely changing out the SEC columns and cleaning the dirty flowcell, it is necessary to run the linear control for each batch of samples in order to correct for minor variations in chromatographic conditions from batch-to-batch.

4.5. Short-chain branching effect correction

In a polyethylene copolymer short-chain branches, such as ethyl, butyl, or hexyl branches, have little effect on the resin's melt rheology, but they do influence its R_g–MW relationship. Intuitively, a copolymer should have a smaller R_g than a homopolymer of the same MW because the overall backbone length of the copolymer is shorter than that of the homopolymer. However, the dimension of a polymer molecule is also influenced by other factors, such as the 'goodness' of the solvent, the interaction between polymer chains and the solvent, and the so-called over-crowding effect [57–59], etc. Because of this complexity, few reliable

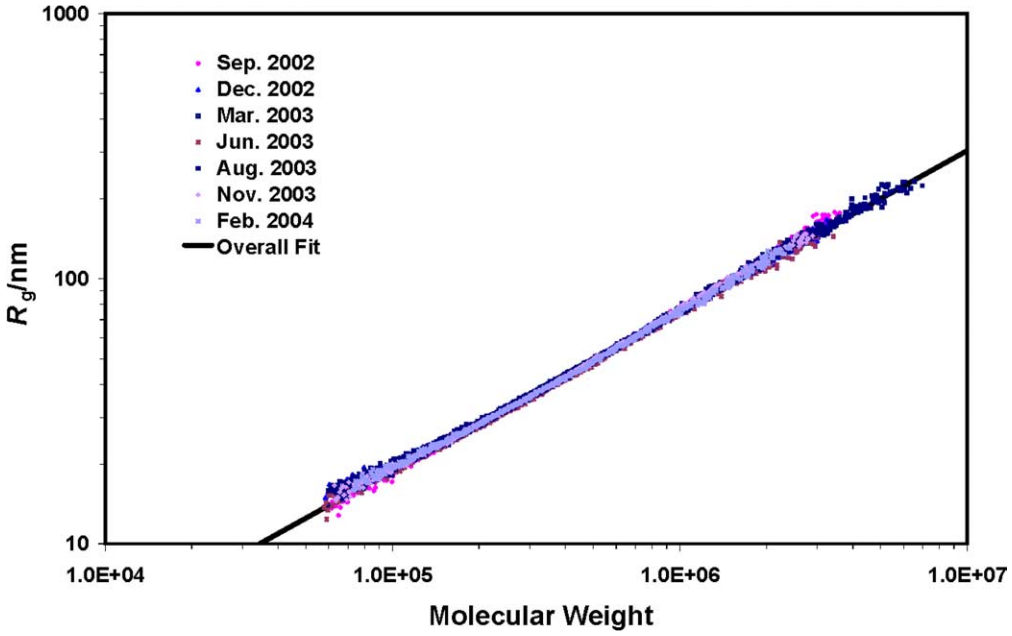

Fig. 10. The relationships of radius of gyration (R_g) and molecular weight for the linear control run over a period of 18 months.

theoretical relationships between R_g and SCB content (x_{SCB}) can be found in the literature. The best way to correct for the SCB effect on R_g is probably still through empirical methods.

Conceptually, to correct the SCB effect on the branching index across the MWD, two relationships are needed. One is the relationship between the branching-index correction factor (Δg_{3w}) and the SCB content (x_{SCB}), and the other is the relationship between SCB content and molecular weight, both of which can be determined experimentally (vide infra). Mathematically, the product of these two relationships gives the branching index correction factor (Δg_{3w}) as a function of MW, as shown in Eq. (19),

$$\frac{d(\Delta g_M)}{d(M)} = \frac{d(x_{SCB})}{d(M)} \frac{d(\Delta g_M)}{d(x_{SCB})} \quad (19)$$

where M represents molecular weight.

To establish the relationship between Δg_{3w} and x_{SCB}, however, one must have PE standards that meet the following criteria: first of all, the standards must not contain any LCB; secondly, they must have known amounts of SCB previously determined via other means, such as NMR or FT-IR; and lastly, SCB in these SCB standards must not be a function of the MWD, meaning they must have flat SCB distributions across their molecular weight distributions.

Polymer standards that meet these criteria are listed in Table 1. Note that all of the SCB standards listed in Table 1 were made with CPChem's proprietary metallocene catalyst technology unless otherwise indicated. They have been evaluated by rheology and found, within the experiment error, to be linear. LCB, if any, was at or below rheology's detection limit. SCB contents as determined via NMR or FT-IR are listed in Table 1. In addition, the SCB distributions across the MWD of these standards were found to be practically flat (Data not shown.).

Fig. 11 is a plot of R_g as a function of molecular weight for these SCB correction standards. Fig. 11 also includes the R_g–MW curve for the linear control for comparison. For clarity, not all of the SCB standards were plotted in the figure. It can be seen that the R_g–MW curves of these SCB correction standards are all parallel to that of the linear control. Linear relationships between log R_g and log M were obtained for all of these SCB correction standards. Within the experimental error, the slopes of these plots in Fig. 11 were found to be virtually the same and equal to 0.595 ± 0.003.

Using Eq. (17a), the relationships of branching index g_{3w} as a function of molecular weight were established. A typical g_{3w}–M plot for a typical SCB correction standard is shown in Fig. 12 for all the SCB correction standards. The value of g_{3w} for the standard was taken from the average of g_{3w} across the MWD. Please note that in order to minimize uncertainties resulted from the normal fluctuation of chromatographic conditions during the experiment, data plotted in Fig. 12 were taken from a combination of g_{3w}–M data sets obtained by referencing multiple runs of the SCB standard to that of the linear control. In this particular case, there were five replicate runs for both the SCB standard and the linear control. Therefore, data plotted in Fig. 12 were a combination of 25 g_{3w}–M data sets for the SCB standard. Note also that manual de-spiking had been performed before the averaging process.

The relationship between the branching index correction factor Δg_{3w} and SCB content (x_{SCB}) for ethylene-1-hexene copolymers is shown in Fig. 13. The SCB correction factor Δg_{3w} is defined as the difference between branching index (g_{3w}) of the linear control (equals to unity) and that of the SCB correction standard. This means that, by adding Δg_{3w} to branching indices g_{3w} of SCB copolymers, g_{3w} of the SCB standards should go back to unity, the linear case, since these SCB correction standards do not contain LCB. After curve fitting with a polynomial, the relationship between branching index correction factor Δg_{3w} and SCB content (x_{SCB}) may be represented by Eq. (20) for ethylene-1-hexene copolymers at the given chromatographic conditions:

$$\Delta g_M = (6.242E-03)x_{SCB} - (8.936E-05)x_{SCB}^2 \quad (20)$$

It should be emphasized that Eq. (20) is applicable only to ethylene-1-hexene copolymers run under the same chromatographic conditions as stated in the Experimental section. Different types of SCB have been found to have

Table 1
Basic characteristics of short-chain branching polyethylene standards used for SBC correction

Sample ID	M_n/1000[a] (g/mol)	M_w/1000[a] (g/mol)	M_w/M_n[a]	MI[b] (g/10 min)	Density[c] (g/cm^3)	SCB Content (# SCB/1000C)
SSEH-A	54.2	121.0	2.23	1.0	0.944	1.1[d]
SSEH-B	55.7	117.1	2.10	0.8	0.935	3.4[d]
SSEH-C	61.0	123.4	2.02	1.0	0.918	10.9[d]
SSEH-D	53.0	92.6	1.75	3.5	0.895	31.0[e]
SSEH-E[f]	51.2	100.1	1.95	2.6	0.896	31.7[d]

[a] Measured via SEC-MALS.
[b] ASTM D1238, condition 190 °C/2.16 kg.
[c] ASTM D1505
[d] Measured via NMR.
[e] Measured via FTIR.
[f] ExxonMobil exact 4150.

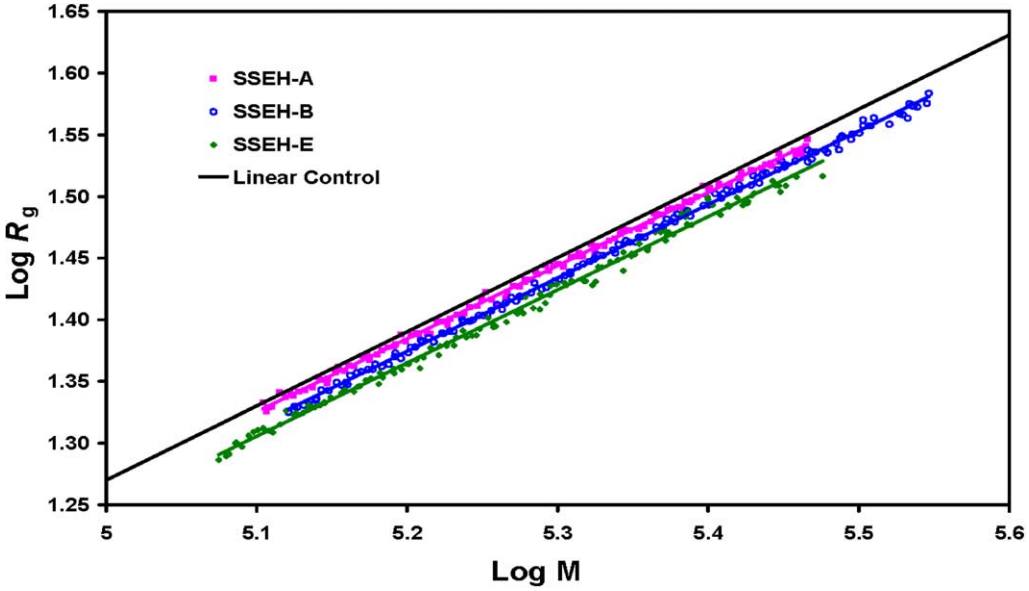

Fig. 11. The relationships of radius of gyration (R_g) as a function of molecular weight for selected SCB correction standards (ethylene/1-hexene copolymers) and the linear control. The slope of these lines is 0.595 ± 0.003.

different branching index correction factors Δg_{3w}. Moreover, chromatographic conditions, such as the flowrates and run temperatures, etc. have also been found to influence the correction factors significantly. Therefore, it is necessary to re-determine the correction factors after any changes to the chromatographic conditions.

4.6. Applications

Examples given in this section are meant to demonstrate how SEC-MALS method was applied to detect LCB in the polyethylene resins listed in Table 2. Samples listed in Table 2 include a high pressure low-density PE (LAS-F), a polyethylene homopolymer (LAS-G) and an ethylene/1-hexene copolymer (LAS-H).

Fig. 14 shows plots of the relationships between R_g and MW for these three samples. R_g–MW for the linear control is also plotted in Fig. 14 for comparison. It can be seen that R_g of all three samples in Fig. 14 show significantly negative deviation from the linear control. Of these three samples, LAS-F showed the highest deviation, LAS-G the least, with LAS-H somewhere in between.

Eq. (16) was employed to convert R_g–MW data plotted in Fig. 14 into branching index g_{3w}–M relationships, which are shown in Fig. 15. In order to convert the branching index g_{3w}–M relationships into LCB frequency as a function of

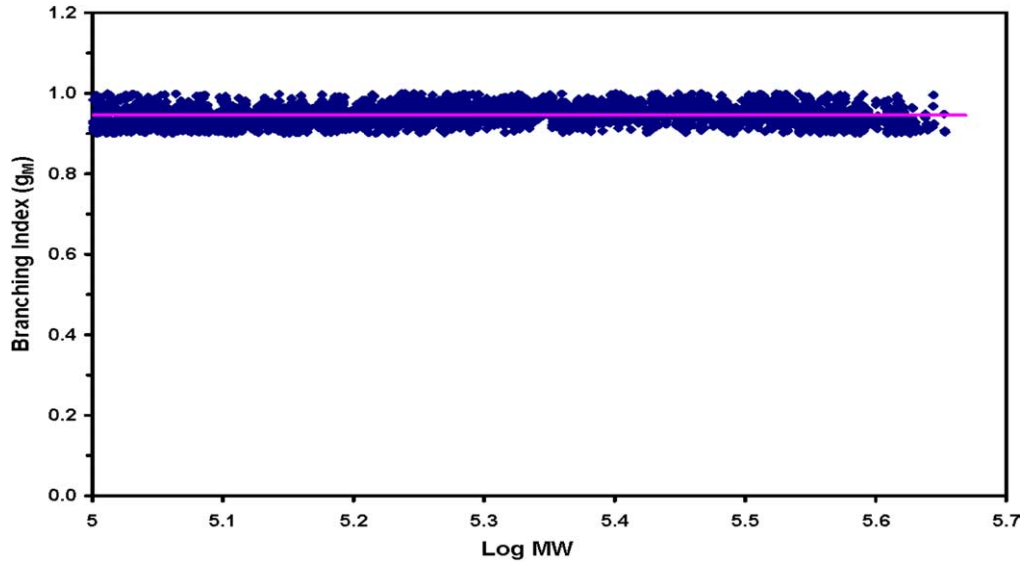

Fig. 12. The relationship between branching index (g_{3w}) and molecular weight for a typical SCB correction standard (SSEH-C) used for SCB effect correction. The polymer contains 10.9 SCB/1000 carbons as determined via NMR. Solid line in the figure represents g_{3w} average for the sample.

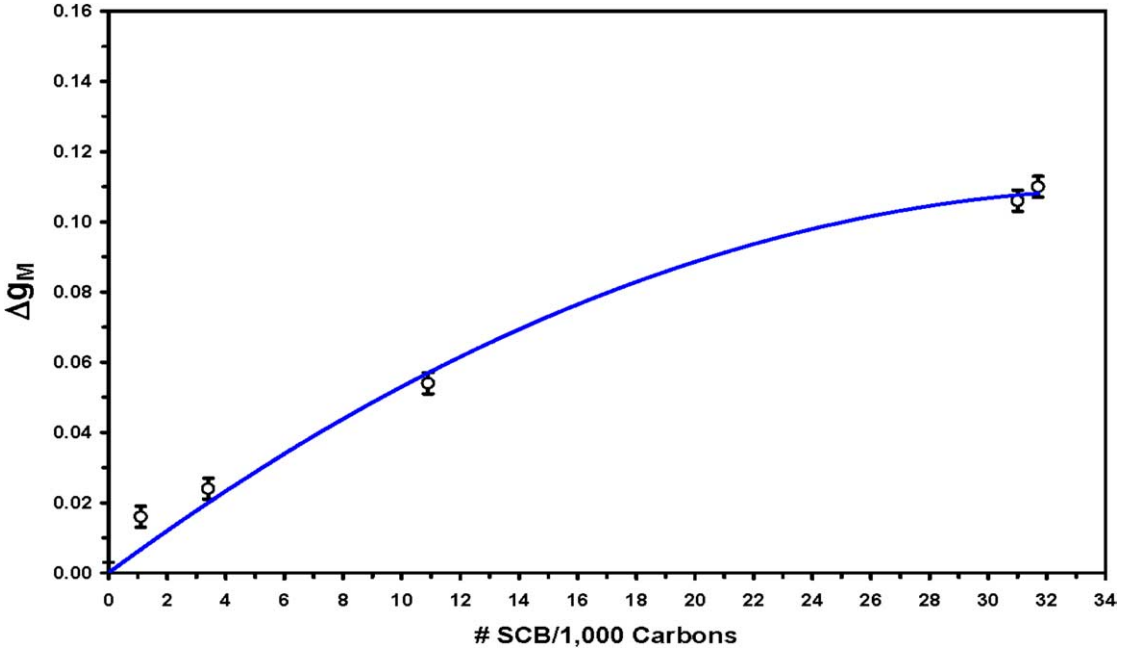

Fig. 13. SCB correction factor Δg_{3w} as a function of SCB content for ethylene-1-hexene copolymers.

molecular weight distribution using Eqs. (17a) and (18), the SCB effect on branching index had to be corrected first for the copolymer LAS-H.

The SCB distribution across the molecular weight distribution (SCBD) profile for LAS-H as determined via the SEC-FTIR technique is shown in Fig. 16. Fitting the experimental data of the SCB content (x_{SCB}) as a function molecular weight, the following relationship was obtained:

$$x_{SCB} = 17.383M^{-0.0433} \quad (21)$$

where M represents the molecular weights. Substituting x_{SCB} in Eq. (20) with Eq. (21) resulted in a relationship between the branching index correction factor Δg_{3w} and the molecular weight for this polymer, which then was used to calculate branching index as a function of molecular weight for the copolymer. The SCB-effect-corrected g_{3w}–M relationship thus obtained is also plotted in Fig. 15. As expected, after the correction of the SCB effect, the g_{3w}–M curve of LAS-H moved up compared to the uncorrected curve.

Profiles of long-chain branching distributions across the molecular weight distributions as calculated by using Eq. (17a) combined with Eq. (18) are shown in Fig. 17. To obtain the relationship between B_{3w} and g_{3w}, in-house LCB calculation software was employed to deduce LCB content per molecule (B_{3w}) from the branching index g_{3w} using Eq. (17a). During the calculation, an iteration is carried out by the software to find the best solution for B_{3w} at each given g_{3w} and molecular weight. For unreasonable data points (i.e. $g_{3w} > 1$) resulting from data fluctuation, their B_{3w} values were automatically set to zero. Finally, LCB frequency was calculated for each molecular weight by substituting B_{3w} thus obtained into Eq. (18).

Of the three samples listed in Table 2, LAS-F, an LDPE sample, showed much higher LCB levels than LAS-G and LAS-H, just as expected. After the SCB correction, LCB frequency in LAS-H was lowered to some extent, but was still generally higher than that in LAS-G. LCB determined via the SEC-MALS method was found to be generally in good agreement with that reported in the literature and/or

Table 2
Basic characteristics of long-chain branched (LCB) polyethylene resins

Sample ID	Type of polymer	M_n/1000[a] (g/mol)	M_w/1000[a] (g/mol)	M_w/M_n[a]	MI[b] (g/10 min)	HLMI[c] (g/10 min)	Density[d] (g/cm^3)
LAS-F	HP LDPE	11.4	444.6	39.0	7	n.a.[e]	0.917
LAS-G	Homopolymer	135.7	483.1	3.6	0	0	0.937
LAS-H	Copolymer	83.0	289.4	3.5	0	0.6	0.914

[a] Measured via SEC-MALS.
[b] ASTM D1238, condition 190 °C/2.16 kg.
[c] ASTM D1238, condition 190 °C/21.6 kg.
[d] ASTM D1505.
[e] Not available.

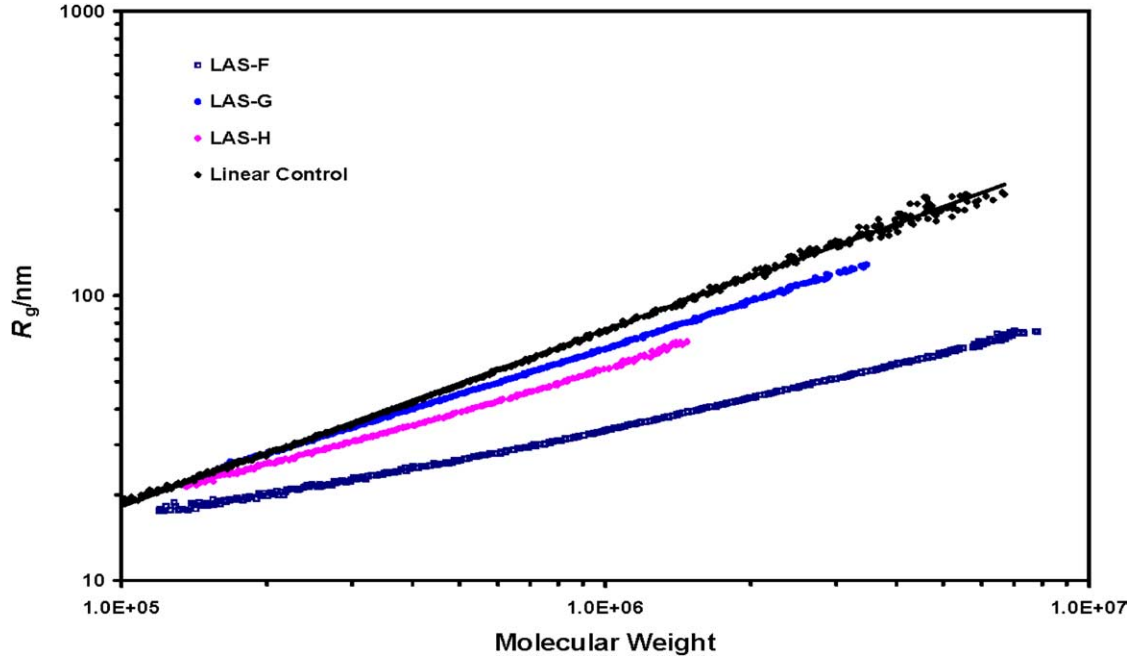

Fig. 14. The relationships between radius of gyration (R_g) and molecular weight for the long-chain branched polymers listed in Table 2.

determined via other LCB methods. Detailed comparison of LCB determined via SEC-MALS method and other methods will be reported elsewhere.

Unlike rheology and NMR methods that measure the average amount of LCB in whole polymers, the SEC-MALS method not only measures the LCB frequency, but also gives information on how LCB is distributed across the molecular weight distribution. As shown in Fig. 17, LCB in LAS-G and LAS-H were not flatly distributed across the molecular weight distribution; they were actually concentrated at the high molecular weight ends and peaked at MW 660,000 and 440,000 g/mol, respectively. LCB in the LDPE was not flatly distributed across the MWD either and was peaked at ca. MW 500,000 g/mol. The LCBD information can be of great importance in understanding the LCB formation mechanism in polyethylene research and development.

The other advantage of the SEC-MALS LCB detection method is that there is virtually no limitation for its application to the high molecular weights. For example, because of its extremely high viscosity, long-chain branched and high molecular weight polymer LAS-G could not be

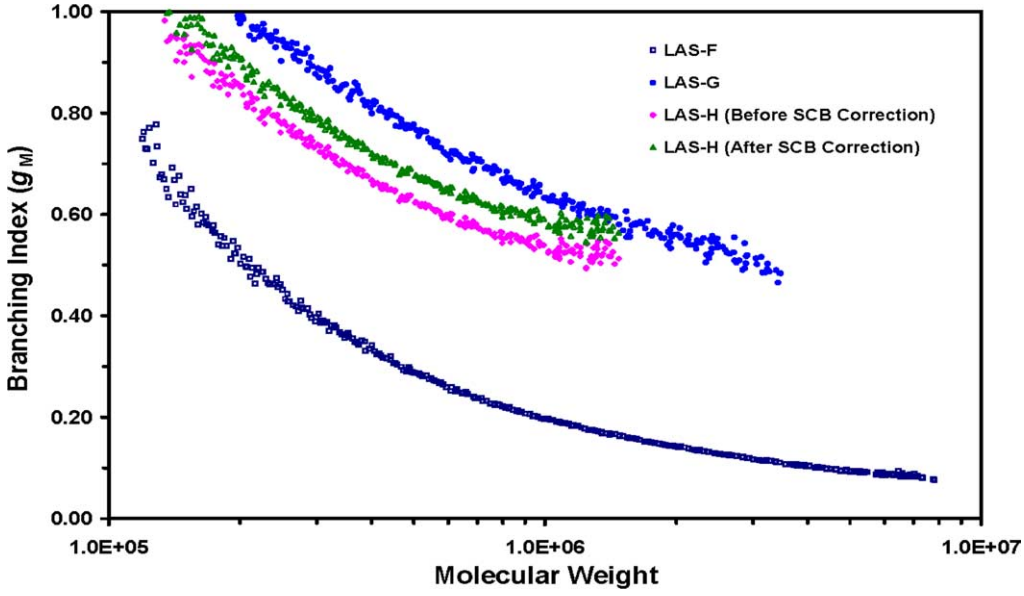

Fig. 15. The relationships between branching index (g_{3w}) and molecular weight for the long-chain branched polymers listed in Table 2, including that for LAS-H before and after SCB correction.

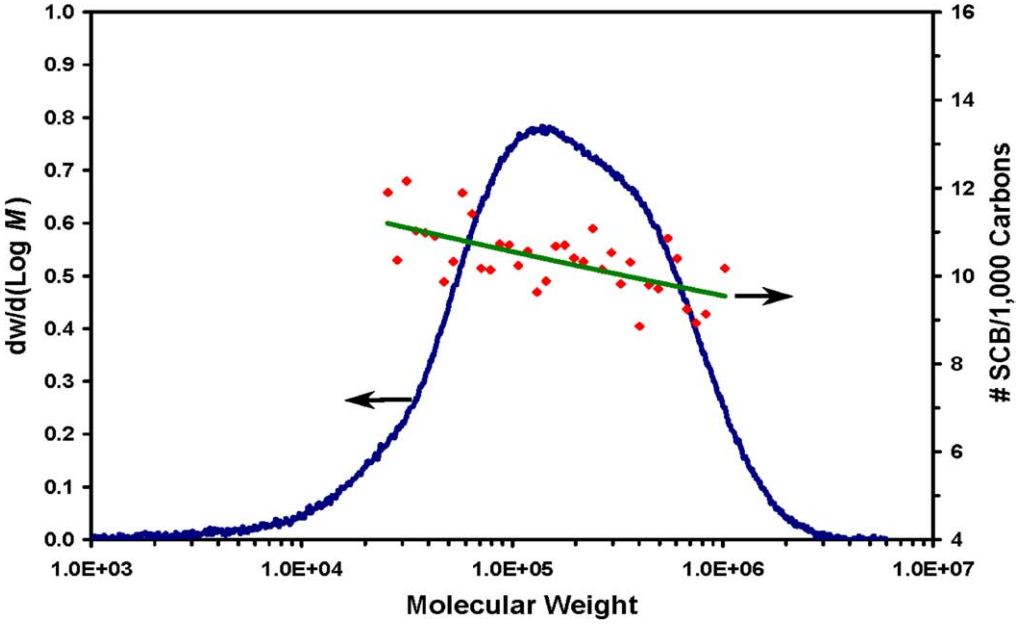

Fig. 16. Short-chain branching distribution across the molecular weight distribution for sample LAS-H.

studied via rheology because its melt was too stiff to be pressed down to the required thickness for rheological measurements. This problem, however, does not exist for SEC-MALS since it measures the solution properties of the polymer. As long as a polymer is soluble, it can be studied via SEC-MALS. In fact, SEC-MALS is more sensitive to detect low levels of LCB in the high molecular weights than it is in the low molecular weights, as can be realized from Figs. 6 and 7.

The SEC-MALS method is, however, not without limitations for LCB determination. First, the SEC-MALS method cannot quantify LCB for low molecular weight polymers. This is because, as already mentioned above, the uncertainty of measured R_g values increases rapidly as the size of the polymer approaches the cut-off molecular weights at which the angular dependence of the scattered light disappears. For the laser of wavelength 690 nm as employed in this report, the smallest R_g detectable is believed to be ca. 10 nm, which translates into MW of ca. 50,000 g/mol for polyethylene provided the concentrations of the low MW components in the polymer in question are high enough to give decent *S*/*N*. In practice, however, the concentrations of low MW components in a whole polymer can never meet the *S*/*N* requirement. If the concentrations

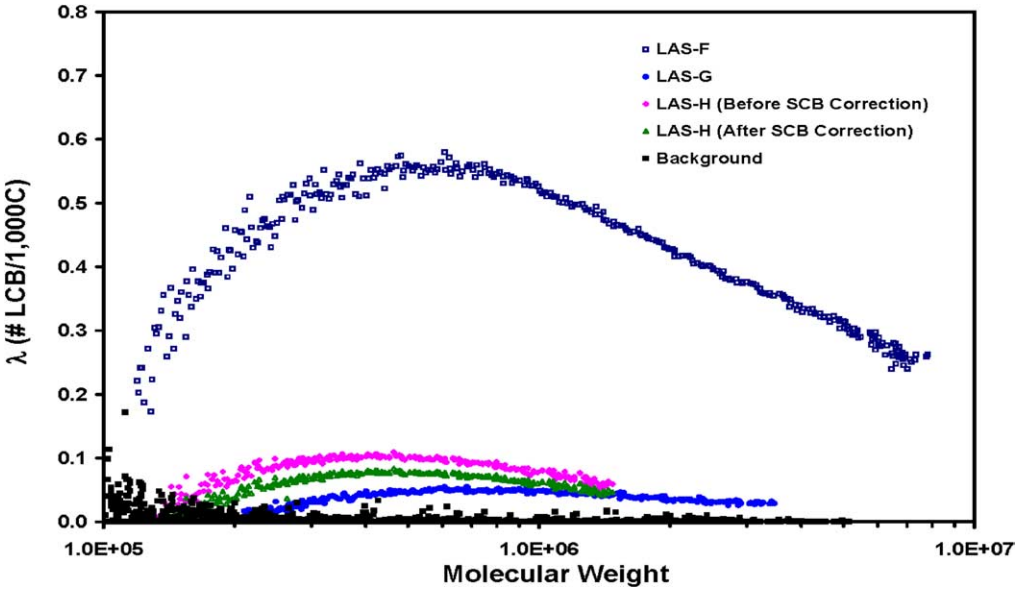

Fig. 17. Long-chain branching distribution across the molecular weight distribution for the long-chain branched polymers listed in Table 2, including that for LAS-H before and after SCB correction.

were that high, the viscosities of the polymer solution would be too high to obtain good quality chromatograms, which would result in poorer detection limit or higher error bars for R_g at the low MW. Secondly, although the SEC-MALS method described in this paper can quantify both LCB contents and LCBD, no information can be given on LCB architectures by this method. Although it has been demonstrated that the architecture, as well as the number, of long chain branches dictates a resin's rheology [60–62], quantitatively determining a polymer's LCB architecture involves a lot of further fundamental research, which is beyond the scope of this study.

5. Conclusions

By combining SEC with the multi-angle light scattering technique (SEC-MALS), a chromatographic method has been established for the determination of long-chain branching and long-chain branching distribution across the molecular weight distribution in polyethylene resins. The following major conclusions are made from this study:

(1) Both long-chain branching content and long-chain branching distribution across the molecular weight distribution can be determined via the SEC-MALS method using the Zimm–Stockmayer approach. The SEC-MALS method can also quantify LCB in polymers that cannot be characterized by other method due to their extremely high melt viscosities caused by very high MW and/or high LCB content.
(2) The SCB effect on the radii of gyration of copolymers can be corrected using an empirical method. Using linear copolymers with known contents of SCB that are flatly distributed across the molecular weight distribution, an empirical relationship between the SCB correction factor as a function of SCB content is established. After the SCB effect correction, LCB in ethylene copolymers can also be determined via the SEC-MALS method.
(3) SEC-MALS is a very sensitive method for LCB determination. It has a higher sensitive for measuring long-chain branching in high molecular weights than in low molecular weights. The determination limit of the SEC-MALS method is molecular weight dependent. For molecular weights equal to or greater than 1,000,000 g/mol, the detection limit is 0.005 LCB/1000 carbons (or 5E-6). As the molecular weight decreases, the sensitivity decreases and LCB must be present at higher levels before it can be detected.
(4) Short-term reproducibility is excellent and long-term stability is very good for this LCB determination method. Both a dirty light scattering flowcell and aged SEC columns can influence the long-term stability.
(5) The background noise in LCB detection is generally low, i.e. lower than 0.01 LCB/1000 carbons ($<$1E-5) for MW equal to or greater than 200,000 g/mol. For molecular weights lower than 200,000 g/mol, the background noise increases rapidly.

Acknowledgements

We would like to thank Dr Steve Wharry for NMR determination, and Mark Stepp and Melvin Hildebrand for technical assistance. We would also like to thank Chevron Phillips Chemical Company LP for allowing the publication of this work.

References

[1] Reodel MJ. J Am Chem Soc 1953;75:6110.
[2] Tung LH. J Polym Sci 1959;36:287.
[3] Hogan JP, Levett CT, Werkman RT. SPE J 1967;23:87.
[4] Small PA. Adv Polym Sci 1975;16:4.
[5] Graessley WW. Acc Chem Res 1977;10:332.
[6] Shroff RN, Sheda M. J Polym Sci A-2 1917;8:1970.
[7] Raju VR, Rachapudy H, Graessley WW. J Polym Sci Polym Phys 1979;17:1223.
[8] Vera JF, Santamaria A, Munoz-Escalona A, Lafuente P. Macromolecules 1998;31:3639.
[9] Malmberg A, Kokka E, Lehmus P, Lofgren B, Seppala JV. Macromolecules 1998;31:8448.
[10] Vega J, Aguilar M, Peon J, Pastor D. e-Polymers 2002;46:1 [and references therein].
[11] Randall JC. J Macromol Sci, Rev Macromol Phys 1989;C29:201.
[12] Yau WW, Hill DR. Int J Polym Anal Charact 1996;2:151.
[13] Wasserman SH, Graessley WW. Polym Eng Sci 1996;36:852.
[14] Lai S-Y, Plumley TA, Butler TI, Knight KW, Kao CI. SPE ANTEC Pap 1994;40:1814.
[15] Shroff RN, Mavridis H. Macromolecules 1999;32:8454. Shroff RN, Mavridis H. Macromolecules 2001;34:7362.
[16] Robertson CG, Garcia-Franco CA, Srinivas S. J Polym Sci, B, Polym Phys 2004;42:1671.
[17] Shaw MT, Tuminello WH. Polym Eng Sci 1996;42:81.
[18] Wood-Adams PM, Dealy JM. Macromolecules 2000;33:7481.
[19] Janzen J, Colby RH. J Mol Struct 1994;485/486:569.
[20] Bird RB, Armstrong RC, Hassager O. Dynamics of polymer liquids. 2nd ed. New York: Wiley; 1987.
[21] Yau WW, Gillespie D. Analytical and polymer science, TAPPI polymers, laminations, and coatings conference proceedings, Chicago 2000;2:699.
[22] Beer F, Capaccio G, Rose LJ. J Appl Polym Sci 1999;73:2807.
[23] Wood-Adams PM, Dealy JM, deGroot AW, Redwine OD. Macromolecules 2000;33:7489.
[24] Zimm BH, Stockmayer WH. J Chem Phys 1949;17:1301.
[25] Zimm BH, Kilb RW. J Polym Sci 1959;37:19.
[26] Debye P, Bueche AM. J Chem Phys 1948;16:573.
[27] Flory PJ. Principles of polymer chemistry. Ithaca, New York: Cornell University press; 1953.
[28] Scholte TH. In: Darwin JV, editor. Developments in polymer characterization, vol. 4. New York: Applied Science; 1983 [chapter 1].
[29] Hadjichristidis N, Xenidou M, Iatrou H, Pitsikalis M, Poulos Y, Avgeropoulos A, et al. Macromolecules 2000;33:2424.
[30] Kaye W, McDaniel JB. Appl Opt 1974;13:1934.
[31] Fox TG, Flory PJ. J Am Chem Soc 1951;73:1904.
[32] Ptitsyn OB, Eizner YuE. Sov Phys Technol Phys 1960;4:1020.
[33] Wyatt PJ. Anal Chim Acta 1993;272:1.

[34] Wintermantel M, Antonetti M, Schmidt M. J Appl Polym Sci, Appl Polym Symp 1993;52:91.
[35] Podzimek S. J Appl Polym Sci 1994;54:91.
[36] Jackson C, Chen Y-J, Mays JW. J Appl Polym Sci 1996;59:179.
[37] Frater DJ, Mays JW, Jackson C. J Appl Polym Sci 1997;35:141.
[38] Pozimek S, Vlecek T, Johann C. J Appl Polym Sci 2001;81:1588.
[39] Rayal U. J Appl Polym Sci 1994;53:1557.
[40] Tackx P, Tacx JCJF. Polymer 1998;39:3109.
[41] Beer F, Capaccio G, Rose LJ. J Appl Polym Sci 1999;73:2807.
[42] Hadjichristidis N, Xenidou M, Iatrou H, Pitsikalis M, Poulos Y, Avgeropoulos A, et al. Macromolecules 2000;33:2424.
[43] Cotts PM, Guan Z, McCord E, McLain S. Macromolecules 2000;33:6945.
[44] Gabriel C, Kokko E, Lofgren B, Seppala J, Munstedt H. Polymer 2002;43:6383.
[45] Yu Y, Rohlfing DC, Hawley GR, DesLauriers PJ. Polym Prepr (Am Chem Soc) 2003;44:50.
[46] Wang W-J, Kharchenko S, Migler K, Zhu S. Polymer 2004;45:6495.
[47] Guttman GM, Maurey JR. NISTIR 1993;5199.
[48] See also: American Polymer Standards Corp, Mentor, OH (www.ampolymer.com). Note: At the run temperature, 145 (C, it was found that d*n*/d*c* was equal to 0.095 ml/g by assuming the refractive index changes linearly as a function of temperature and that the polymer standard is 100% soluble.
[49] Debye PJ. Appl Phys 1944;15:338.
[50] Zimm BH. J Phys Chem 1945;13:141. Zimm BH. J Phys Chem 1948;16:1093.
[51] Huglin MB. Light scattering from polymer solutions. New York: Academic Press; 1972.
[52] Note: we choose the words 'linear control' instead of 'linear standard' to reflect the fact that this polymer is not necessarily strictly linear. However, it is linear enough that we shall call it 'essentially linear'. It is not trivia to find a truly linear sample as the standard.
[53] Arnett RL, Thomas CP. J Phys Chem 1980;84:649.
[54] Raju VR, Rachapudy H, Graessley WW. J Polym Sci, Part A2 1979;17:1223.
[55] Pearson DS, Ver Strate G, Von Meerwall E, Schilling FC. Macromolecules 1987;20:1133.
[56] Pearson DS, Fetters LJ, Graessley WW, Ver Strate G, Von Meerwall E. Macromolecules 1994;27:711.
[57] Mandelkern L. In: Mark JE, editor. Physical properties of polymers, 2nd ed. Washington DC: American Chemical Society; 1993 [chapter 4].
[58] Scholte TG, Meijerink NLJ, Schoffeleers NM, Brands AMG. J Appl Polym Sci 1984;29:3763.
[59] Press WH, Flannery BP, Teukolsky SA, Vettering WT. Numerical recipes. Cambridge, England: Cambridge University Press; 1986.
[60] McLeish TCB, Larson RG. J Rheol 1998;42:81.
[61] Larson GR. Macromolecules 2001;34:4556.
[62] Lohse DJ, Milner ST, Fetters LJ, Xenidou M, Hadichristidis N, Mendelson RA, et al. Macromolecules 2002;35:3006.